View metadata, citation and similar papers at core.ac.uk

brought to you by CORE

provided by IntechOpen

We are IntechOpen, the world's leading publisher of Open Access books Built by scientists, for scientists

4,800
Open access books available

122,000
International authors and editors

135M
Downloads

Our authors are among the

154
Countries delivered to

TOP 1%
most cited scientists

12.2%
Contributors from top 500 universities

CLARIVATE ANALYTICS BOOK CITATION INDEX INDEXED

WEB OF SCIENCE™

Selection of our books indexed in the Book Citation Index in Web of Science™ Core Collection (BKCI)

Interested in publishing with us?
Contact book.department@intechopen.com

Numbers displayed above are based on latest data collected.
For more information visit www.intechopen.com

9

Waveguide Photodiode (WGPD) with a Thin Absorption Layer

Jeong-Woo Park
Electronics and Telecommunications Research Institute
Republic of Korea

1. Introduction

Surface illumination photodiode (PD) shows the tradeoff between quantum efficiency and transit time. This is because a thin absorber region is required for a short carrier transit time whereas a thick absorber region is required for high quantum efficiency. In order to achieve good quantum efficiency the absorption region should be ~2μm, which results in a transit time bandwidth of <12GHz. Waveguide photodiodes can overcome this limitation because the thickness of the absorbing region has little effect on the internal quantum efficiency if the absorber region is long enough. WGPDs, in which the quantum efficiency and transit time are decoupled, can overcome this restriction. In this type of devices, the external quantum efficiency is determined principally by the input coupling efficiency because the internal quantum efficiency can close to 100%.

Coupling into WGPDs can be broadly categorized as side-illumination and evanescent coupling. In Figure 1, three types of coupling scheme for WGPDs are shown. Those include a) side illumination type, b) evanescent coupling type, and c) side illumination with a thin absorption/core region. For side illumination, light is focused directly onto the edge of the absorbing layer. With this approach, a responsivity of 0.85A/W and 50-GHz bandwidth has been reported (K. Kato *et al*, 1992). In the report, he used a multimode waveguide in a transverse direction to acquire a higher coupling efficiency than in a typical p-i-n structure. A primary disadvantage of this type of device is poor optical power capability compared to evanescent coupling approach. Evanescently-coupled photodiodes have demonstrated responsivity up to 0.75A/W with a bandwidth of 42GHz (F. Xia *et al*, 2001). As another evanescently-coupled photodiode, an etched short multimode graded index waveguide approach has shown a responsivity of 0.96A/W and 40GHz bandwidth (T. Takeuchi *et al*, 2001). A similar approach that integrates a short planar diluted waveguide with an etched input facet has shown 0.73A/W responsivity and 47GHz bandwidth (M. Achouche *et al*, 2003). The responsivity of 1.02A/W and 48GHz bandwidth has been achieved with a short multimode input waveguide that consists of a diluted waveguide and two optical matching layers (S. Demiguel *et al*, 2003).

In this chapter, a new WGPD with a thin absorption layer will be introduced. Also, methods of design and optimizations for this new type of WGPD are described. A responsivity of 1.08A/W was achieved at 1550nm wavelength, which corresponds to an external quantum efficiency of 86.4% with TE/TM polarization dependence less than 0.25dB. For the same device, the bandwidth was ~40GHz. Also, nonlinearity of the device was characterized.

Source: Advances in Optical and Photonic Devices, Book edited by: Ki Young Kim,
ISBN 978-953-7619-76-3, pp. 352, January 2010, INTECH, Croatia, downloaded from SCIYO.COM

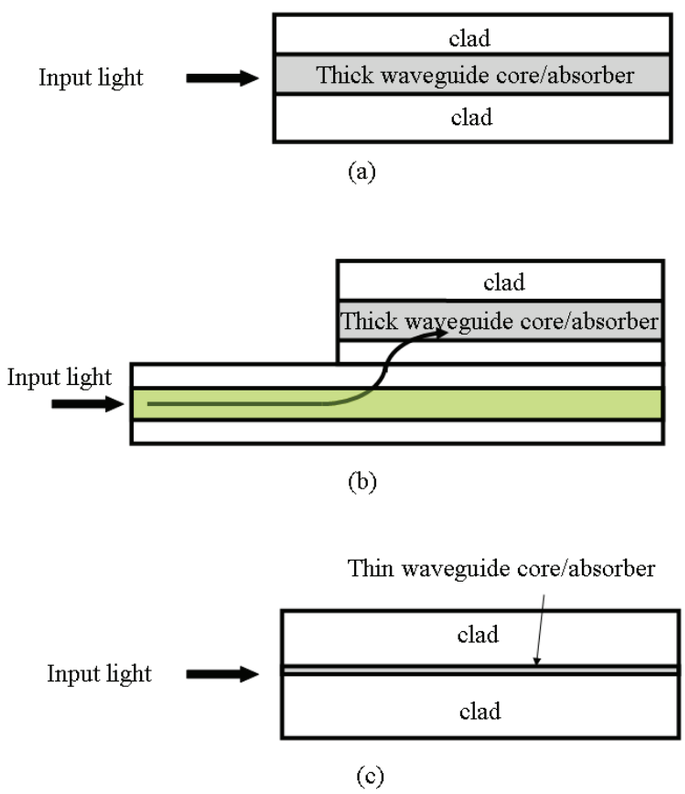

Fig. 1. three types of coupling scheme for WGPDs. a) side illumination, b) evanescent coupling, and c) side illumination with a thin absorption/core region.

2. High responsivity

The guided mode of a waveguide with thin core layer has a larger beam size than that with thick core layer as indicated in Figure 2. This property can be profitably applicable to InP based high responsivity WGPD. Figure 2 shows simulated beam size of guided mode for waveguide structure with InGaAs core/InGaAsP(λg=1.4μm) clad and InGaAs core/InP clad. Beam size is defined at the point, at which field amplitude is reduced down to *1/e* of its maximum amplitude. As shown in Figure 2, for core thickness of less than 0.2μm, guided beam size is enlarged.

The enlarged beam size is well matched with other large sized waveguide, such as optical fiber, silica planar waveguide, or polymer planar waveguide. This property can be applied to overcoming the beam size mismatch between InP based semiconductor waveguides and other waveguides such as optical fiber, silica planar waveguide, or polymer planar waveguide. Using a thin core layer, optical coupling between WGPDs and external waveguides can also enhance a external quantum efficiency, or responsivity.

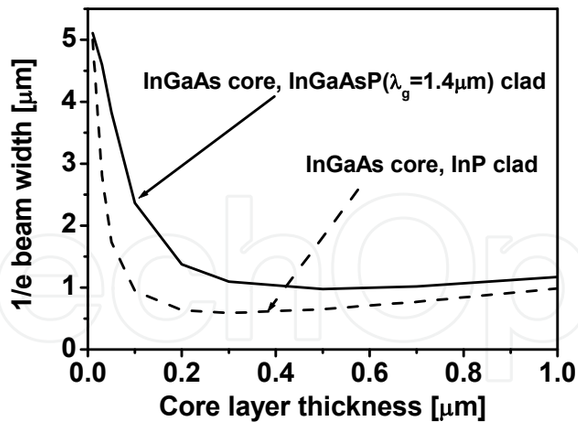

Fig. 2. Two dimensional simulated beam sizes (field amplitude is down to *1/e* of maximum amplitude) for InGaAs core, InGaAsP(λ_g=1.4μm) core and InP clad.

For conform of high coupling efficiency between optical fiber and WGPDs with a thin core layer, four types of WGPDs were fabricated and responsivity for each devices were measured. Figure 3 shows waveguide structures of four different types of WGPDs. Total undoped layer surrounding InGaAs absorption layer was 0.6μm thick for each type of WGPDs. Mesa etching was done past to absorption layer to define deep ridge waveguide. After polyimide passivation and contact opening, Ti/Pt/Au p-electrode was evaporated and rapid-annealed. After Ti/Pt/Au n-electrode evaporation, rapid-annealing were performed. After cleavage, each WGPDs are anti-reflection-coated. Widths of input facet waveguides were 20μm.

Table (I) shows measured responsivity with coupling of lensed fiber and flat-ended fiber. First, responsivity measured at the wavelength of 1550nm, was 0.815A/W for Type (II), which was 300μm long. The calculated vertical mode coupling efficiency, η_v was 65% for Type (II). Horizontal mode coupling efficiency, η_h, is 100% because width of WGPD is wider than that of flat-ended fiber. Thus, total coupling efficiency, $\eta=\eta_h\eta_v$, is 65%. The coupling efficiency of 65% is corresponding to responsivity of 0.81A/W, which well agrees with measured responsivity of 0.815A/W. For Type (II), polarization dependency was less than 0.25dB. This value of less than 0.25dB is originated from different coupling efficiency between TE and TM mode input. Another WGPD with absorption layer thickness of 0.2μm shows similar polarization dependency of 0.25dB. This indicates that 300Å thick absorption layer have a bulk absorption behavior rather than quantum well absorption behavior.

However, Type (I), which has 100Å thick absorption layer thickness, shows quantum well absorption behavior. Figure 4 shows the polarization dependent responsivity curve. For comparison, polarization dependency of Type (II) is drawn together. In Figure 4, x-axis is ε, the parameter on Poincarè sphere, which represents the linear polarization state of input light and y-axis is normalized responsivity with respect to maximum responsivity, in dB unit. The calculated TE/TM difference of coupling efficiency for Type (I) is 0.202dB. Thus, polarization dependency of Type (I), shown in Figure 4, is originated from absorption coefficient difference between TE and TM mode. The comparison of polarization dependence for Type (I) and Type (II) indicates that WGPD with thin absorption layer should have more than 100Å thick absorption layer for polarization independent operation.

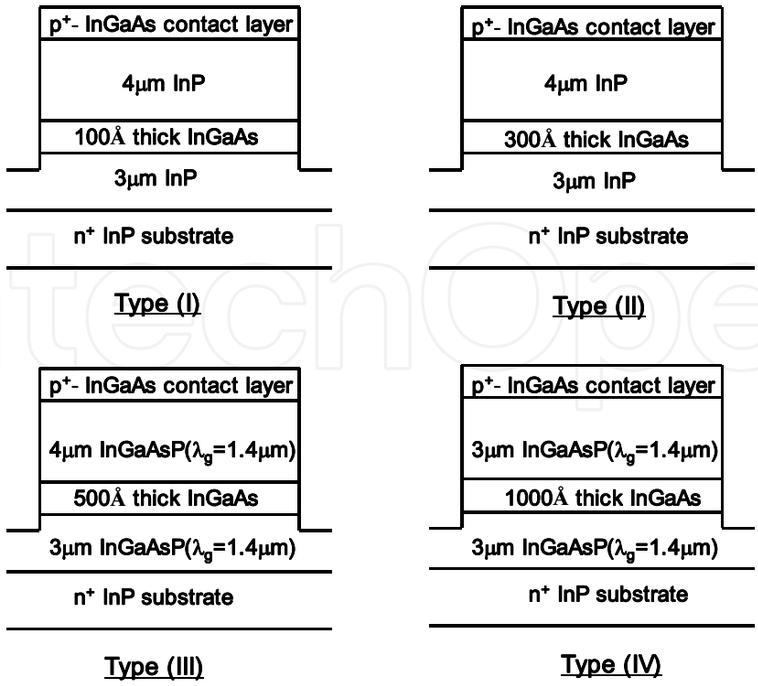

Fig. 3. Tested WGPD structures for high responsivity operation.

PD type	Responsivity (flat-ended fiber)	Responsivity (lensed fiber)
(I)	Polarization dependent	Polarization dependent -
(II)	0.815A/W	1.09A/W
(III)	0.93A/W	1.09A/W
(IV)	0.76A/W	1.08A/W

Table (I) Responsivities for four types of WGPDs

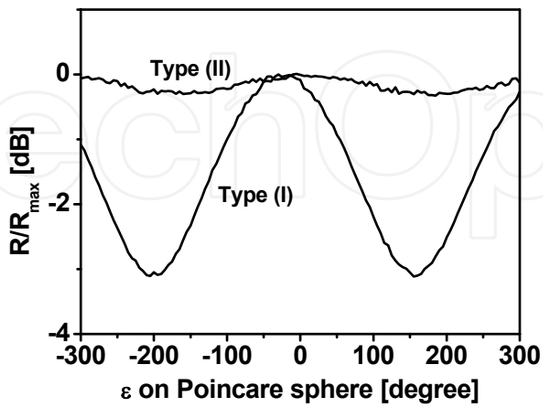

Fig. 4. Polarization dependencies of Type (I) and Type(II).

Another drawback of WGPD with 100Å thick absorption layer is low coupling efficiency, which is contradictory to the simulated value. For type (I), the calculated coupling

efficiency, coupled with flat-ended fiber, is 82.6%, which corresponds to responsivity of 0.99A/W for the wavelength of 1490nm. Measured responsivity, however, implies that coupling efficiency of Type (I), when coupled with flat-ended fiber, is 30.6% and maximum responsivity is 0.368A/W for the input wavelength of 1490nm.

To measure the coupling efficiency of Type (I), responsivities of PDs with different lengths were measured for TE input light. Figure 5 shows responsivity values versus PD length. This data was fitted with Equation (1).

$$R = \frac{C \cdot \lambda}{1.24} \cdot (1 - e^{-\alpha \cdot \Gamma \cdot L}) \quad (1)$$

In Equation (1), R, C, λ, α, Γ, and L are responsivity, coupling efficiency, input wavelength, absorption coefficient of absorption layer, confinement factor of guided beam within a absorber, and PD length, respectively.

Fitting results indicate that coupling efficiency is 30.6% and $\alpha\Gamma$ is 0.00511μm^{-1}. Low responsivity for Type (I) was conformed by measuring five PDs. Five PDs show almost same responsivity. Discrepancy between simulated value and measured one can be explained by weakly guiding structure of Type (I). It is estimated that 100Å thick core layer is too thin to support the propagation of light through total waveguide. Even a small perturbation of waveguide structure such as side wall roughness may induce waveguide to be leaky for 100Å thick core layer.

Type (III) shows responsivity of 0.93A/W, when coupled with non-lensed flat fiber. Type (III) has low index difference between clad and core. Thus, guided mode is more spread than the case of high core/clad index difference like Type (II). Calculated beam size of Type (III) is 3.83μm. Compared to the calculated beam size of 2.81μm for Type (II), more enlarged beam size of Type (III) is more similar to mode size of flat fiber, which gives higher responsivity. Polarization dependency of Type (III) is also smaller than 0.25dB, showing bulk absorption property. Comparison of Type (II) and Type (III) shows that small index difference between core and clad is more advantageous, for high responsivity.

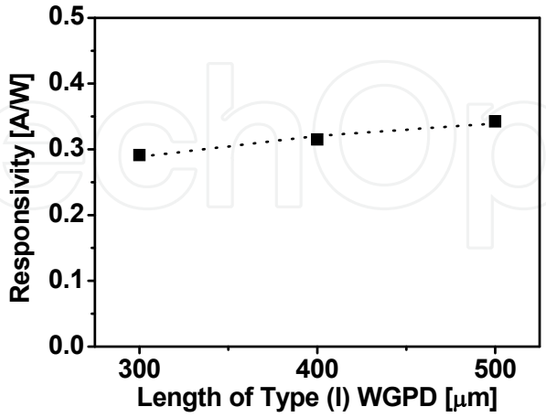

Fig. 5. Responsivity versus PD length of Type (I). Fitting was done by Eq. (1)

Type (IV) with 1000Å absorption layer thickness and 70μm length shows responsivity of 0.76A/W coupled with flat fiber and 1.08A/W coupled with lensed fiber at a wavelength of

1550nm. Calculated guiding mode size of Type (IV) is 2.36μm, which is small compared to 3.83μm of Type (III). Smaller guided mode size of Type (IV), originated from thicker core layer than Type (III), gives more mode-mismatch and smaller responsivity than Type (III).

2. Bandwidth property

To find out time dependent current of photodiode, displacement current should be considered. Including displacement current and photo-generated current, time dependent current of photodiode is given by Equation (2), according to (G. Lucovsky *et al*, 1964).

$$I_{photodiode}(t) = \frac{\frac{1}{L}\int_0^L [I_{drift,e}(x,t) + I_{drift,h}(x,t)]dx}{1 + j \cdot \omega \cdot R \cdot C} \tag{2}$$

In Equation (2), $I_{drift,e}(x,t)$, $I_{drift,h}(x,t)$, R and C are photo-generated electron and hole drift current at (x,t), (series resistance of PD+load resistance) and (photodiode capacitance + stray capacitance), respectively. Transit-time limited response is extracted by developing numerator of Equation (2). To calculate transit-time limited frequency response of WGPDs with thin absorption layer, $I_{drift,e}(x,t)$ shown in Figure 6 should be known first.

Assuming input light can be expressed as $P_o \cdot \exp(j \cdot \omega_m \cdot t)$, where P_o, ω_m are amplitude of input beam and modulation frequency, respectively, electron current at x is given by Equation (3).

$$i_{drift,e}(x,t) = R \cdot P_o \cdot \exp[j \cdot \omega_m \cdot (t - \frac{x}{v_e})] \tag{3}$$

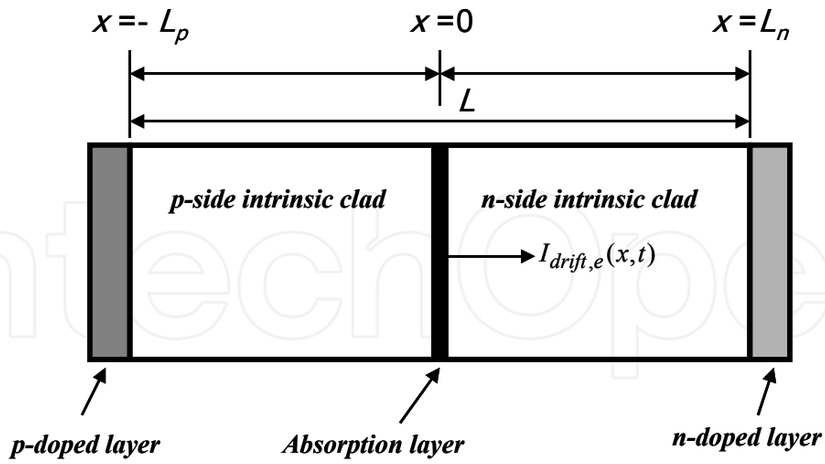

Fig. 6. Configuration for derivation of transit-time limited frequency response of WGPD having thin absorption layer.

In derivation of Equation (3), it is assumed that photocurrent is generated only at x=0. The generated electrons at x=0 drift forward to n-doped region and drift current at x is delayed waveform with respective to current at x=0, with time delay of x/v_e. In Eq.(3), R and v_e are responsivity, electron drift velocity in n-side clad layer, respectively.

Including hole current contribution, the transit-time limited time-dependent photodiode current is given by Equation (4).

$$i_{photodiode}(t) = R \cdot P_o \cdot \exp(j \cdot \omega_m \cdot t) \cdot [\frac{1 - \exp(-j \cdot \omega_m \cdot \frac{L_n}{v_e})}{j \cdot \omega_m \cdot \frac{L}{v_e}} + \frac{1 - \exp(-j \cdot \omega_m \cdot \frac{L_p}{v_h})}{j \cdot \omega_m \cdot \frac{L}{v_h}}] \tag{4}$$

In Equation (4), v_h is hole drift velocity in p-side clad layer. At optimized condition, electron transit time and hole transit time are equal. This condition can be expressed by $L_n / v_e = L_p / v_h = \tau$. At optimized condition, right most term in Equation (4) can be re-written by Equation (5).

$$\begin{aligned} &[\frac{1 - \exp(-j \cdot \omega_m \cdot \tau)}{j \cdot \omega_m \cdot \frac{L_n + L_p}{v_e}} + \frac{1 - \exp(-j \cdot \omega_m \cdot \tau)}{j \cdot \omega_m \cdot \frac{L_n + L_p}{v_h}}]] \\ &= \frac{1 - \exp(-j \cdot \omega_m \cdot \tau)}{j \cdot \omega_m \cdot \tau} \end{aligned} \tag{5}$$

Transit time limited bandwidth, f_t, is defined as the frequency at which absolute value of Equation (5) is equal to $1/\sqrt{2}$, and can be calculated as

$$f_t \cong \frac{2.8}{2\pi\tau} \tag{6}$$

Including transit time limitation and RC effect, bandwidth of photodiode, f_{3dB}, is given by Equation (7) with an error of less than 5%(K. Kato *et al*, 1993).

$$\frac{1}{f_{3dB}^2} = \frac{1}{f_t^2} + \frac{1}{f_{RC}^2} \tag{7}$$

Figure 7 shows the expected 3dB bandwidth with intrinsic layer thickness variation. Considered structures is Type (IV) of which absorption layer thickness is 1000Å. In calculations, The relative dielectric constant and electron drift velocity of InGaAsP (λ_g=1.4μm) was assumed as 11.16 (S. Adachi, 1982) and 1.5X10^{6}cm/sec (A. Galvanauskas et *al*, 1988). Hole velocity was assumed as the half of the electron velocity. In the calculations, PD length was 70μm and PD width was tapered from 5μm to 1μm. A 70μm length is sufficient for responsivity of more than 1.0A/W for a 3μm mode size fiber. Also, series resistance, Rs and load resistance were assumed as 5Ω and 50Ω.

As can be seen Figure 7 (a), optimized point for maximum bandwidth with pad capacitance of zero, is the point at which RC limited bandwidth and carrier transit-time limited bandwidth are same. At this optimized point, bandwidth can be a 120GHz even though thin absorption layer needs long absorption length of 70μm which is two or three times long compared to typical high-speed WGPDs. When pad capacitance of 10fF is included, however, bandwidth is reduced and optimum point is shfited as can be seen in Figure 7(b).

Based on simulated results of Figure 7 (a), (b), WGPD with a 1000Å thick absorber was fabricated. The thickness of intrinsic layer on n-electrode side and p-electrode side were

0.6μm and 0.3μm, respectively. Width of WGPD was tapered from 5μm to 1μm and length was 70μm. The frequency response of a device was measured using an impulse response. The optical impulse from femto-second laser was applied to WGPD. The impulse response was converted to bandwidth curve using fourier transform. Figure 8 shows the bandwidth response at -3V bias, after the de-embedding the RF loss of the measurement system. The RF losses of measurement system include those of probe, bias tee, cable, and DC block. As can be seen from the Figure 8, bandwidth of ~42GHz was obtained. Hole-trapping at the hetero-interface of i-InGaAsP(λ_g=1.4μm)/i-InGaAs can be a bandwidth limiting factor. However, the bandgap discontinuity at i-InGaAsP(λ_g=1.4μm)/i-InGaAs does not degrade the bandwidth significantly.

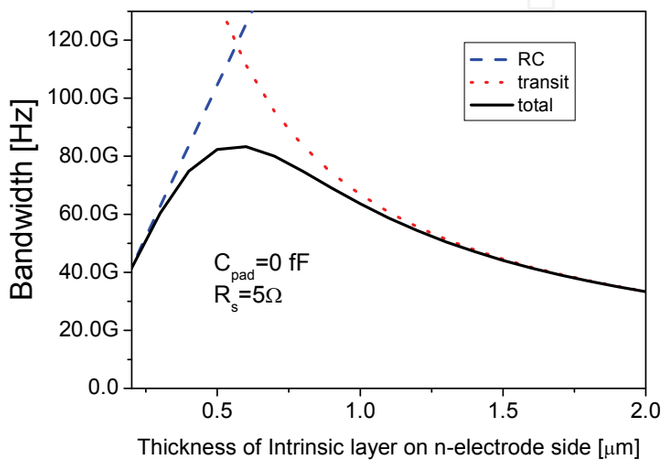

(a)

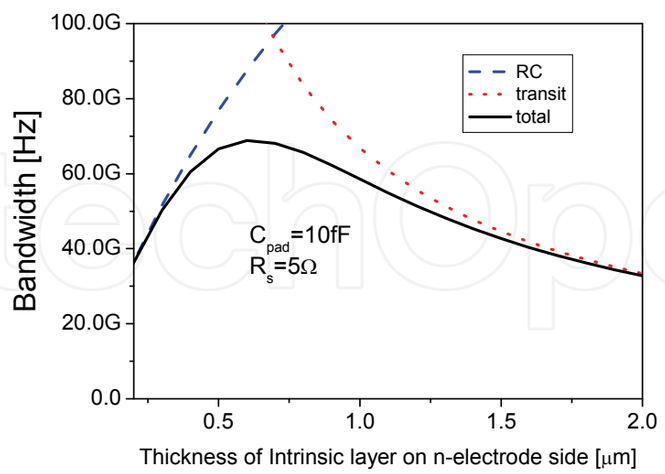

(b)

Fig. 7. RC limited, transi-time limited and total bandwidth traces with variations of thickness of n-side intrinsic layer (a) without consideration of pad capacitance (b) with the pad capacitance of 10fF.

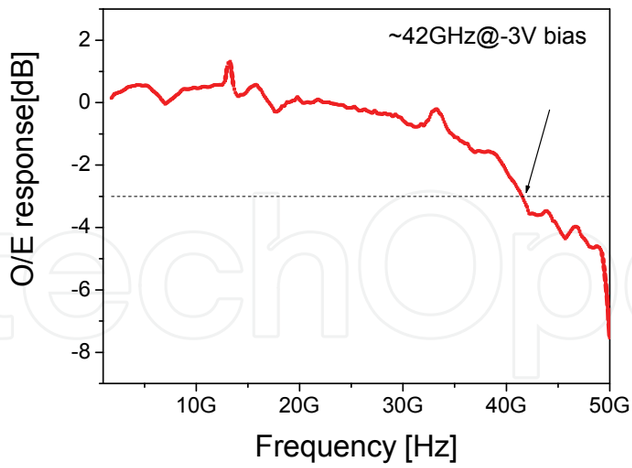

Fig. 8. A measured frequency response of WGPD with a thin absorption layer of 1000Å.

3. Intermodulation distortion properties

In some optical communication systems such as fiber-optic community antanna television (CATV) systems, many optical signals with different modulation frequencies are inputted to a PD. In this case, non-linearity properties of PD should be supressed to re-generate elctrical signals from optical signals without distortions.

When a device shows nonlinear response, input-output relation is represented as shown in Figure 9. An output can be expressed as polymomials of input signal. With this nonlinear relations, supurious outputs of which frequencies are f2+f1, f2-f1, 2f1-f2, 2f2-f1... can be generated when sinusoidal inputs of which frequencies are f1, f2, ..., are applied to device.

These supurious outputs should be filtered out not to influence on original signals with

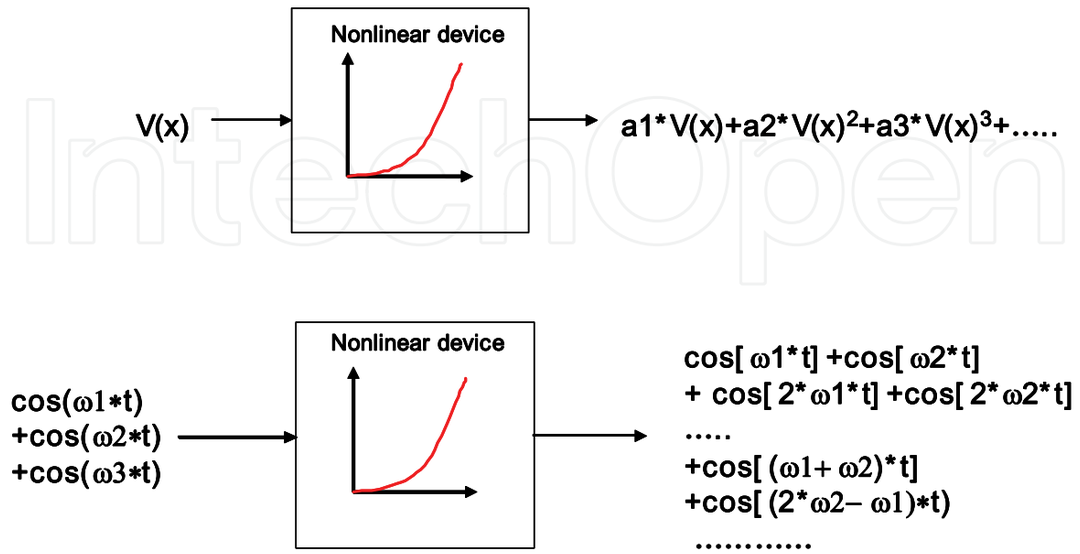

Fig. 9. Supurious signals from nonlinear devices

frequencies of f1, f2,.... As can be seen in Figure 10, however, frequencies of some supurious outputs are close to frequencies of original signal. These supurious signals cannot be filtered out and quality of converted signals from optical to electrical is degraded. The degree of degradations is determined by linearity of PD. The second order intermodulation products of two signals at f1 and f2 occur at f1+f2, f2-f1, 2·f1 and 2·f2. The third order intermodulation products of two signals at f1 and f2 would be at 2·f1+f2, 2·f1-f2, f1+2·f2, and 2·f2-·f1. Among these products, signals at f1+f2, 2·f1-f2 and 2·f2-·f1 are not filtered out. Therefore, to obtain high purity signal among many signals, signals at f1+f2, 2·f1-f2 and 2·f2-·f1 should be supressed when optical-to-electrical conversion occurs at PD. Signals at f2+f1 and f2-f1 are the 2nd order intermodulation distortion (IMD2). Signals at 2·f1-f2 and 2·f2-·f1 are the 3rd order intermodulation distortion (IMD3). The ratio of each intermoulation signal to original signal should be as small as possible and the ratio is expressed with unit of dBc.

The main source of nonlinearity of PD is a space charge induced nonlinearity (K. J. Williams *et al*, 1996), (Y. Kuhara *et al*, 1997). The photo-generated carriers induce space charges in a intrinsic layer of PD. Carrier-dependent carrier velocities associated with a perturbed electric filed due to space-charge and loading effect are main source of photodetector nonlinear behavior. The amount of space-charge generated from photocurrents depends on the power density of incident optical signal. The smaller a density of photo-currents are, the smaller nonlinarity of PD are. To reduce a IMD2 and IMD3, a density of photo-generated carriers should be reduced. WGPDs with thin absorption layer can have a suppressed nonlinearity because thin absorption layer with a long absorption length produce a reduced density of photo-carriers.

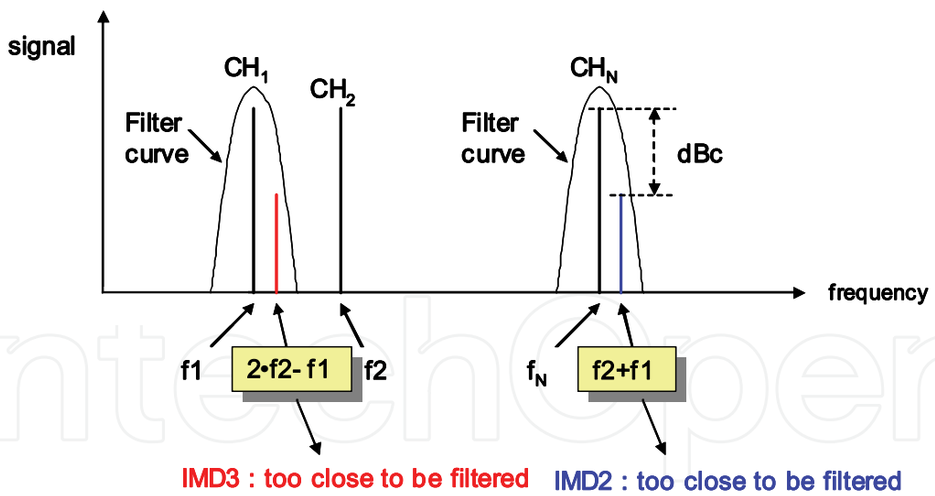

Fig. 10. Intermodulation signals close to original signals. IMD2 and IMD3 signals are too close to original signal to be filtered out

In Figure 11, IMD2 and IMD3 characteristics are presented for a Type (IV) WGPD with width of 10μm and length of 70μm. Its -3dB bandwidth was ~20GHz. The device shows IMD2 of less than -70dBc for a DC photocurrent of 1mA, optical modulation index(OMI) of 0.7 and 50Ω load. Also, IMD3 was less than -90dBc for the same conditions. IMD3 for a voltage range of -6~-8V cannot be measured because IMD3 at that range is too small to be detected within the limit of spectrum analyzer sensitivity.

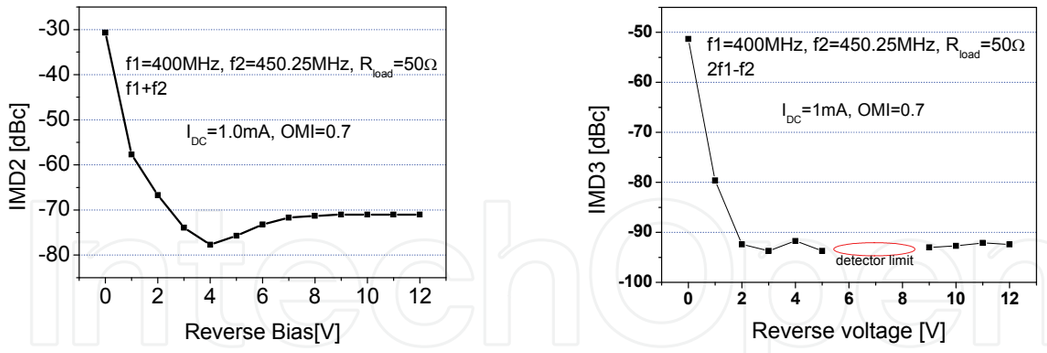

(a)IMD2 (b)IMD3

Fig. 11. IMD2 and IMD3 characteristics of a Type (IV) WGPD

4. Conclusion

A new WGPD with a thin absorption layer was introduced. Methods of design and optimizations for this new type of WGPD were described. Absorber should be thicker than 100Å to obtain a high responsivity and low polarization dependency. A responsivity of 1.08A/W was achieved at 1550nm wavelength, which corresponds to an external quantum efficiency of 86.4% with TE/TM polarization dependence less than 0.25dB. For the same device, the bandwidth of ~40GHz was obtained. The formula for the transit-time limited frequency response of this kind of devices was obtained. With this formula, optimization of frequency response is possible. Also, this kind of devices can show a suppressed nonlinearity.

5. References

K. Kato, S. Hata, K. Kawano, J. Yoshida, and A. Kozen, (1992), *IEEE J. of Quantum Elect.* Vol. 28, No. 12, pp. 2728-2735.

F. Xia, J. K. Thomson, M. R. Gokhale, P. V. Studenkov, J. Wei, W. Lin, and S. R. Forrest, (2001), *IEEE Photon. Tech. Lett.* Vol. 13, No. 8, pp. 845-847

T. Takeuchi, T. Nakata, K. Makita, and T. Torikai, *Proceedings of OFC 2001*, Vol.3, Paper WQ2-1.

M. Achouche, S. Demiguel, E. Derouin, D. Carpentier, F. Barthe, F. Blache, V. Magnin, J. Harari, and D. Decoster, *Proceedings of OFC 2003*, Paper WF5.

S. Demiguel, N. Li, X. Li, X. Zheng, J. Kim, J. C. Campbell, H. Lu, and K. A. Anselm, (2003), *IEEE Photon. Tech. Lett.* Vol. 15, No.12, pp. 1761-1763.

G. Lucovsky, R. F. Schwarz, and R. B. Emmons, (1964) *J. of Applied Phys.*, Vol.35, No.3, pp. 622-628.

K. Kato, S. Hata, K. Kawano, and A. Kozen, (1993), *IEICE. Trans. Electron.*, Vol. E76-C, No. 2, pp. 214-221.

S. Adachi, (1982), *J. of Applied Phys.*, vol.53 , pp. 8775-8792.

A. Galvanauskas, A. Gorelenok, Z. Dobrovol'skis, S. Kershulis, Yu. Pozhela, A. Reklaitis, N. Shmidt, (1988), *Sov. Phys. Semicond.*, Vol.22, pp.1055-1058.

K. J. Williams, R. D. Esman, and M. Dagenais, (1996), *.J. of Lightwave Tech.*,Vol. 14, No. 1, pp.84~96.

Y. Kuhara, Y. Fujimura, N. Nishiyama, Y. Michituji, H. Terauchi, and N. Yamabayashi, (1997), *.J. of Lightwave Tech.*,Vol. 15 No. 4, pp.636~641

IntechOpen

IntechOpen

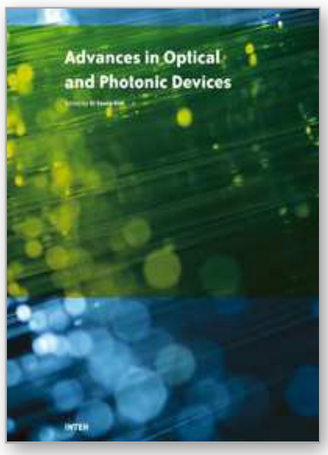

Advances in Optical and Photonic Devices

Edited by Ki Young Kim

ISBN 978-953-7619-76-3
Hard cover, 352 pages
Publisher InTech
Published online 01, January, 2010
Published in print edition January, 2010

The title of this book, Advances in Optical and Photonic Devices, encompasses a broad range of theory and applications which are of interest for diverse classes of optical and photonic devices. Unquestionably, recent successful achievements in modern optical communications and multifunctional systems have been accomplished based on composing “building blocks” of a variety of optical and photonic devices. Thus, the grasp of current trends and needs in device technology would be useful for further development of such a range of relative applications. The book is going to be a collection of contemporary researches and developments of various devices and structures in the area of optics and photonics. It is composed of 17 excellent chapters covering fundamental theory, physical operation mechanisms, fabrication and measurement techniques, and application examples. Besides, it contains comprehensive reviews of recent trends and advancements in the field. First six chapters are especially focused on diverse aspects of recent developments of lasers and related technologies, while the later chapters deal with various optical and photonic devices including waveguides, filters, oscillators, isolators, photodiodes, photomultipliers, microcavities, and so on. Although the book is a collected edition of specific technological issues, I strongly believe that the readers can obtain generous and overall ideas and knowledge of the state-of-the-art technologies in optical and photonic devices. Lastly, special words of thanks should go to all the scientists and engineers who have devoted a great deal of time to writing excellent chapters in this book.

How to reference
In order to correctly reference this scholarly work, feel free to copy and paste the following:

Jeong-Woo Park (2010). Waveguide Photodiode (WGPD) with a Thin Absorption Layer, Advances in Optical and Photonic Devices, Ki Young Kim (Ed.), ISBN: 978-953-7619-76-3, InTech, Available from: http://www.intechopen.com/books/advances-in-optical-and-photonic-devices/waveguide-photodiode-wgpd-with-a-thin-absorption-layer

INTECH
open science | open minds

InTech Europe
University Campus STeP Ri
Slavka Krautzeka 83/A
51000 Rijeka, Croatia
Phone: +385 (51) 770 447

InTech China
Unit 405, Office Block, Hotel Equatorial Shanghai
No.65, Yan An Road (West), Shanghai, 200040, China
中国上海市延安西路65号上海国际贵都大饭店办公楼405单元
Phone: +86-21-62489820

Fax: +385 (51) 686 166
www.intechopen.com

Fax: +86-21-62489821

IntechOpen

IntechOpen

© 2010 The Author(s). Licensee IntechOpen. This chapter is distributed under the terms of the Creative Commons Attribution-NonCommercial-ShareAlike-3.0 License, which permits use, distribution and reproduction for non-commercial purposes, provided the original is properly cited and derivative works building on this content are distributed under the same license.

IntechOpen

IntechOpen